JACC: CARDIOVASCULAR INTERVENTIONS
VOL. 2, NO. 10, 2009

ISSN 1936-8798/09/$36.00
PUBLISHED BY ELSEVIER INC.
DOI: 10.1016/j.jcin.2009.07.012

Intravascular Ultrasound Assessment of the Incidence and Predictors of Edge Dissections After Drug-Eluting Stent Implantation

Xuebo Liu, MD, Kenichi Tsujita, MD, PHD, Akiko Maehara, MD, Gary S. Mintz, MD, Giora Weisz, MD, George D. Dangas, MD, PHD, Alexandra J. Lansky, MD, Edward M. Kreps, MD, LeRoy E. Rabbani, MD, Michael Collins, MD, Gregg W. Stone, MD, Jeffrey W. Moses, MD, Roxana Mehran, MD, Martin B. Leon, MD

New York, New York

Objectives We used intravascular ultrasound (IVUS) to assess incidence, predictors, morphology, and angiographic findings of edge dissections after drug-eluting stent (DES) implantation.

Background DES implantation strategies differ compared with bare-metal stenting; coronary dissections after DES implantation have not been well studied.

Methods We studied 887 patients with 1,045 non–in-stent restenosis lesions in 977 native arteries undergoing DES implantation with IVUS imaging.

Results Eighty-two dissections were detected; 51.2% (42 of 82) involved the proximal and 48.8% (40 of 82) the distal stent edge. Residual plaque area (8.0 ± 4.3 mm^2 vs. 5.2 ± 3.0 mm^2, $p < 0.0001$); plaque burden ($52.2 \pm 11.7\%$ vs. $36.2 \pm 15.3\%$, $p < 0.0001$); plaque eccentricity (8.4 ± 5.5 vs. 4.0 ± 3.4, $p < 0.0001$); and stent edge symmetry (1.2 ± 0.1 vs. 1.1 ± 0.1, $p = 0.02$) were larger; plaque burden $\geq$50% was more frequent (62.0% vs. 17.2%, $p < 0.0001$); calcium deposits (52.1% vs. 35.2%, $p = 0.03$) more common; and lumen-to-stent-edge-area ratio (0.9 ± 0.2 vs. 1.0 ± 0.2, $p < 0.0001$) was smaller in the edge dissection group compared with the nondissection group. Intramural hematomas occurred in 34.1% (28 of 82) of dissections. When compared with nonhematoma dissections, residual plaque and media area (6.4 ± 2.5 mm^2 vs. 8.9 ± 4.6 mm^2, $p = 0.04$) was smaller, and stent edges less asymmetric (1.1 ± 0.1 vs. 1.2 ± 0.1, $p = 0.009$) in the dissection with hematoma group. Independent predictors of any stent edge dissection were residual plaque eccentricity (odds ratio [OR]: 1.4, $p = 0.02$), lumen-to-stent-edge-area ratio (OR: 0.0, $p = 0.007$), and stent edge symmetry (OR: 1.2, $p = 0.02$ for each 0.01 increase).

Conclusions IVUS identified edge dissections after 9.2% of DES implantations. Residual plaque eccentricity, lumen-to-stent-edge-area ratio, and stent edge symmetry predicted coronary stent edge dissections. Dissections in less diseased reference segments more often evolved into an intramural hematoma. (J Am Coll Cardiol Intv 2009;2:997–1004) © 2009 by the American College of Cardiology Foundation

From the Columbia University Medical Center and Cardiovascular Research Foundation, New York, New York.
Manuscript received February 14, 2009; revised manuscript received July 21, 2009, accepted July 25, 2009.

JACC: CARDIOVASCULAR INTERVENTIONS, VOL. 2, NO. 10, 2009
OCTOBER 2009:997–1004

Coronary dissections after percutaneous coronary intervention are associated with an increased risk of major adverse cardiovascular events (1). In the bare-metal stent (BMS) era, there was a tendency to minimize stent length to reduce restenosis—even if some disease was left uncovered. This strategy likely impacted on the frequency and severity of edge dissections. Drug-eluting stent (DES) implantation strategies differ from BMS and include gentler pre-dilation, more limited use of debulking devices, treatment of more complex lesions, and covering the lesion 'from normal-to-normal' resulting in use of longer stents. However, the question of whether this strategy impacts on the occurrence of stent edge dissections has not been well studied. Using intravascular ultrasound (IVUS), we assessed the incidence, predictors, morphology, and angiographic findings of edge dissections after DES implantation.

Abbreviations and Acronyms

BMS = bare-metal stent(s)
CI = confidence interval
CSA = cross-sectional area
DES = drug-eluting stent(s)
EEM = external elastic membrane
IVUS = intravascular ultrasound
OR = odds ratio
P and M = plaque and media
PES = paclitaxel-eluting stent(s)
SES = sirolimus-eluting stent(s)

Methods

Patient population and procedure. From November 2004 to March 2006, 887 patients with 1,045 non–in-stent restenosis lesions in 977 native arteries underwent DES implantation with IVUS imaging. There were 722 sirolimus-eluting-stent (SES)-treated lesions (Cypher, Cordis, Miami Lakes, Florida) and 323 paclitaxel-eluting-stent (PES)-treated lesions (Taxus, Boston Scientific, Maple Grove, Minnesota). All studies were reviewed to identify patients with post-stent implantation edge dissections; dissections that occurred after pre-dilation or post-dilation were excluded. This study was approved by the institutional review board; written informed consent was obtained from all patients.

Patient demographics were confirmed by hospital chart review. Coronary risk factors included diabetes mellitus (diet-controlled, oral agent, and insulin-treated), hypertension (medication-treated only), and hypercholesterolemia (medication-treated or a measured total cholesterol >240 mg/dl). Unstable angina was defined as new-onset severe angina, accelerated angina, or angina at rest. Previous myocardial infarction, bypass surgery, and percutaneous coronary intervention were tabulated.

Coronary angioplasty and stenting were performed, and stent size and length selected to fully cover the diseased segment with adequate stent expansion. Pre-dilation or post-dilation was performed at the discretion of the operator. At the beginning of the procedure, a bolus of bivalirudin was administered at a dose of 0.75 mg/kg to achieve an activated clotting time ≥250 s after which an intravenous infusion of 1.75 mg/kg/h was given. Glycoprotein IIb/IIIa inhibitors were used electively or as bail-out at the discretion of the operator.

Angiographic analysis. Dissections were interpreted by experienced interventional cardiologists blinded to the IVUS findings according to the National Heart, Lung, and Blood Institute criteria (2). A significant stenosis was defined as a diameter stenosis >50%. A new stenosis was a new narrowing without adjacent dissection that persisted after the administration of intracoronary nitroglycerin. Haziness was the presence of lucencies within the arterial lumen, not fulfilling the criteria for thrombus. Severe calcification was radio-opacity noted without cardiac motion before contrast injection generally involving both sides of the arterial wall. Extremely angulated segments had a lesion bend >90°.

IVUS imaging and analysis. All IVUS studies were performed after intracoronary administration of 100 to 200 μg nitroglycerin. Only one commercially available IVUS system (Boston Scientific, Fremont, California) was used. The IVUS catheter was advanced >10 mm distal to the lesion, and imaging was performed using an automatic pullback device through to the proximal reference at a pullback speed of 0.5 mm/s. When the first run was ambiguous, additional manual or automated pullbacks, typically with contrast or saline injection, were performed. IVUS data were recorded onto a high-resolution, one-half inch, s-VHS tape or CD for later offline analysis.

Qualitative IVUS analysis was performed according to the criteria of the American College of Cardiology Clinical Expert Consensus Document on Standards for Acquisition, Measurement and Reporting of Intravascular Ultrasound Studies (3). Dissections were tears in the plaque parallel to the vessel wall with visualization of blood flow in the false lumen (confirmed, if necessary, with saline or contrast injection). Intramural hematomas, variants of a dissection, were an accumulation of hyperechoic and homogeneous blood within the medial space that was visually continuous with the intima (or plaque) and adventitia typically with a crescent shape and straightening of the internal elastic membrane.

Using planimetry software (EchoPlaque, INDEC Systems, Mountain View, California), the following pre-intervention and post-intervention measurements were made at proximal and distal stent edge and at the proximal and distal reference segments: external elastic membrane (EEM) cross-sectional area (CSA), lumen CSA, plaque and media (P and M) (P and M = EEM minus lumen) CSA, plaque burden (P and M divided by EEM), and stent CSA. Pre-intervention measurements (corresponding to the stent edges) were made after matching pre- and post-stent IVUS images using branch points, characteristic calcifications, plaque shapes, stent edge, and known pullback speed of the trans-

Table 1. Baseline Clinical and Angiographic Characteristics (n = 82)

Age (yrs)	65.6 ± 11.8
Men (%)	53 (64.6)
Diabetes mellitus (%)	21 (25.6)
Hypertension (%)	60 (73.2)
Hypercholesterolemia (%)	74 (90)
Smoker (%)	32 (39.0)
Unstable angina (%)	26 (31.7)
Previous MI (%)	18 (22.0)
Previous PCI (%)	35 (42.7)
Previous bypass surgery (%)	5 (6.1)
Multivessel disease (%)	75 (91.5)
Type B_2 or C (%)	55 (67.1)
Severe calcification (%)	19 (23.2)
Extremely angulated lesion (%)	8 (9.8)

MI = myocardial infarction; PCI = percutaneous coronary intervention.

ducer. The length of the dissection and/or hematoma was calculated from the known pullback speed (0.5 mm/s × seconds). Plaque eccentricity was maximum/minimum plaque thickness; eccentric plaque had a maximum/minimum plaque thickness >2.0. Stent edge asymmetry was defined as maximum/minimum stent diameter.

Reference sites were the most normal looking cross sections (maximum lumen with minimum plaque) within 5 mm proximal and distal to the stented segment. The image slice with the smallest lumen and greatest plaque within 5 mm proximal and distal to stent edge was also identified and measured. "Normal vessel wall" was defined as having <0.3 mm of intimal thickness. Significant residual plaque burden was defined as ≥50% after stent deployment.

Statistical analysis. Statistical analysis was performed using SAS 9.1 (SAS Institute Inc., Cary, North Carolina). Continuous variables (presented as mean ± 1 SD) were compared using paired or unpaired, 2-sided Student *t* test. Categorical variables (presented as frequencies) were compared using chi-square statistics or Fisher exact test. A p value <0.05 was considered significant. Multivariable conditional logistic regression analysis was performed to determine independent predictors of DES edge dissection.

Results

Among 887 patients (1,045 nonrestenotic lesions in 977 arteries) reviewed for this study, there were a total of 82 stent edge dissections. The incidence of edge dissection was 9.2% per patient (82 of 887), 8.4% per artery (82 of 977), and 7.8% per lesion (82 of 1,045). Baseline clinical demographics and angiographic characteristics are shown in Table 1.

Overall, 51.2% (42 of 82) of the dissections were located at the proximal stent edge; and 48.8% (40 of 82) were

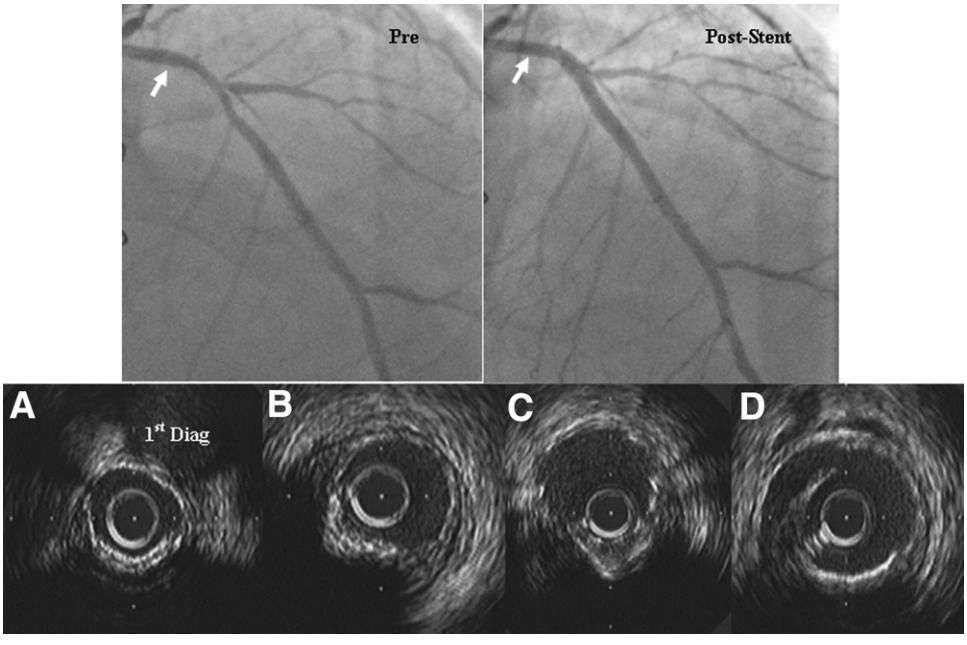

Figure 1. Stent Edge Dissection

Post-stenting, angiography showed a normal appearance at the proximal stent edge (**arrows** indicate dissection site on the pre- and post-stent angiograms). However, intravascular ultrasound demonstrated stent edge dissection. **(A)** Minimum luminal site before stenting. **(B)** The site of proximal stent edge before stenting. **(C)** Proximal stent edge; stent cross-sectional area measured 6.6 mm^2 with stent symmetry of 1.3. **(D)** Stent edge dissection with an arc of approximately 90°, but no lumen compromise.

JACC: CARDIOVASCULAR INTERVENTIONS, VOL. 2, NO. 10, 2009
OCTOBER 2009:997–1004

Table 2. IVUS Findings Comparing Edge Dissection With Opposite Edge Without a Dissection

	Dissection Site (n = 71)	Opposite Edge Without a Dissection (n = 71)	p Value
Peri-stent minimum lumen site			
Plaque morphology (%)			0.31
Normal	2 (3)	4 (6)	
Soft	9 (13)	12 (17)	
Fibrous	40 (56)	40 (56)	
Calcific	10 (14)	7 (10)	
Mixed	10 (14)	8 (11)	
Calcium deposit (%)	37 (52.1)	25 (35.2)	0.03
EEM CSA (mm^2)	14.8 ± 5.1	13.7 ± 4.2	0.20
Lumen CSA (mm^2)	6.7 ± 2.0	8.6 ± 2.9	<0.0001
P and M CSA (mm^2)	8.0 ± 4.3	5.2 ± 3.0	<0.0001
Plaque burden (%)	52.2 ± 11.7	36.2 ± 15.3	<0.0001
Plaque burden >50% (%)	51 (62.0)	12 (17.2)	<0.0001
Plaque eccentricity	8.4 ± 5.5	4.0 ± 3.4	<0.0001
LD/SED	0.9 ± 0.1	1.0 ± 0.1	<0.0001
LA/SEA	0.9 ± 0.2	1.0 ± 0.2	<0.0001
Most normal looking reference			
P and M CSA (mm^2)	6.3 ± 3.6	4.7 ± 2.9	0.004
Plaque burden (%)	42.1 ± 11.7	32.2 ± 14.2	<0.0001
LD/SED	1.0 ± 0.2	1.0 ± 0.1	0.02
LA/SEA	1.0 ± 0.2	1.1 ± 0.2	0.008
Stent edge asymmetry	1.2 ± 0.1	1.1 ± 0.1	0.02

CSA = cross-sectional area; EEM = external elastic membrane; IVUS = intravascular ultrasound; LA = lumen area; LD = mean lumen diameter; P and M = plaque and media; SEA = stent edge area; SED = mean stent edge diameter.

located at the distal stent edge. No patient had dissections at both stent edges.

The distribution of the dissection sites by vessel was 59.8% (49 of 82) in the left anterior descending artery, 18.3% (15 of 82) in the left circumflex artery, 20.7% (17 of 82) in the right coronary artery, and 1.2% (1 of 82) in the left main coronary artery. The incidence of dissection per lesion was 8.3% (49 of 587) in the left anterior descending artery, 7.4% (15 of 204) in the left circumflex artery, 7.9% (17 of 215) in the right coronary artery, and 2.6% (1 of 39) in the left main coronary artery.

There were 60 (74%, 60 of 82) SES-induced dissections and 22 (26%, 22 of 82) PES-induced dissections. The incidence of SES-induced dissections was 8.3% per lesion (60 of 722), and the incidence of PES-induced dissections was 6.2% per lesion (20 of 323, p = 0.26). Intramural hematomas occurred in 34.1% (28 of 82) of the dissections.

Procedural and angiographic findings. Nominal stent diameter (3.2 ± 0.3 mm vs. 3.2 ± 0.5 mm, p = 0.8), stent length (26.6 ± 16.3 mm vs. 21.1 ± 9.1 mm, p = 0.11), maximum balloon size (including the post-dilation balloon, 3.4 ± 0.4 mm vs. 3.3 ± 0.6 mm, p = 0.6), and maximum dilation pressure (including post-dilation inflation pressure, 15.6 ± 3.5 atm vs. 17.2 ± 2.8 atm, p = 0.17) were similar in proximal versus distal dissections, respectively.

Dissections were characterized as type A in 25.6% (21 of 82), type B in 7.3% (6 of 82), type C in 17.1% (14 of 82), and type D to F in 11% (9 of 82). However, 39% (32 of 82) of the dissections were not detected by angiography appearing, instead, as a new stenosis in 20.7% (17 of 82), angiographic haziness in 13.4% (11 of 82), and normal in 4.9% (4 of 82).

IVUS findings in dissections. Eighty-three percent (68 of 82) of edge dissections occurred in eccentric plaque, 14.6% (12 of 82) in concentric plaque, and 2.4% (2 of 82) in a near-normal segment of artery wall. The morphology of the dissection site plaque was hypoechoic in 12.2% (10 of 82), hyperechoic noncalcific in 58.5% (48 of 82), calcific in 13.4% (11 of 82), and mixed in 13.4% (11 of 82). Superficial calcium was detected at 52.5% of the dissection sites with 76% of these calcifications involving the tear in the plaque.

Most (80.5%, 66 of 82) of the dissections occurred at or near the junction of thinnest plaque and normal vessel wall in eccentric plaques; 15.9% (13 of 82) occurred within the plaque (with 12 dissections occurring in the thinnest region of the concentric plaques); and 3.6% (3 of 82) occurred within an arc of normal vessel wall. The direction of the dissection plane was toward the plaque in eccentric lesions and toward the thickest plaque in concentric lesions (Fig. 1).

Table 3. Differences Between Proximal Edges With Versus Without a Dissection and Between Distal Edges With Versus Without a Dissection

Peri-Stent Minimum Lumen Site	Proximal Dissection (n = 37)	Proximal Edge Without Dissection (n = 34)	p Value
Calcium deposit (%)	24 (64.9)	13 (38.2)	0.02
P and M CSA (mm^2)	9.9 ± 3.7	5.3 ± 2.6	<0.0001
Plaque burden (%)	56.8 ± 11.3	35.5 ± 14.5	<0.0001
Plaque eccentricity	8.4 ± 6.1	3.9 ± 3.7	<0.0001
LD/SED	0.9 ± 0.1	1.0 ± 0.1	<0.0001
LA/SEA	0.9 ± 0.2	1.1 ± 0.2	<0.0001
Plaque burden >50% (%)	27 (73.0)	4 (11.8)	<0.0001
Stent edge asymmetry	1.2 ± 0.1	1.1 ± 0.1	0.08
	Distal Dissention (n = 34)	**Distal Edge Without Dissection (n = 37)**	
Calcium deposit (%)	14 (41.2)	12 (32.4)	0.44
P and M CSA (mm^2)	6.5 ± 3.8	5.0 ± 3.4	0.09
Plaque burden (%)	48.5 ± 11.5	36.5 ± 16.0	0.001
Plaque eccentricity	8.5 ± 4.8	4.1 ± 3.1	<0.0001
LD/SED	0.9 ± 0.1	1.0 ± 0.1	0.004
LA/SEA	0.8 ± 0.2	1.0 ± 0.2	0.003
Plaque burden >50% (%)	18 (52.9)	8 (21.6)	0.008
Stent edge asymmetry	1.2 ± 0.1	1.1 ± 0.1	0.21

Abbreviations as in Table 2.

In 4.9% (4 of 82) of the dissections, the depth of the dissection could not be assessed by IVUS due to severe calcification. Otherwise, 11.5% (9 of 78) of the dissections were limited to the intima or atheroma, 83.4% (65 of 78) extended into the media, and 5.1% (4 of 78) extended to the EEM.

The length of the dissections was 5.6 ± 3.2 mm, with no difference between proximal versus distal edge dissections (5.4 ± 3.2 mm vs. 5.8 ± 3.2 mm, p = 0.65).

Seventy-one (87%, 71 of 82) dissections had both pre- and post-intervention IVUS images; 46 were pure dissections, and 25 were dissections with hematomas. Edges with a dissection were first compared with opposite edges without a dissection (Table 2). When measured at the peri-stent minimum lumen site: 1) residual P and M area, plaque burden, and P and M eccentricity were larger in edges with dissections versus opposite edges without dissections; 2) the ratio of mean lumen diameter and area to mean edge stent diameter and area were smaller in the dissection group; 3) significant (≥50%) plaque burden and calcium deposits were more common; and 4) the stent edge was less symmetric. Similar findings were seen when comparing proximal edges with versus without a dissection and when comparing distal edges with versus without a dissection (Table 3).

IVUS findings in intramural hematomas. The incidence of intramural hematomas was 3.2% per patient (28 of 887), 2.9% (28 of 977) per artery, and 2.7% per lesion (28 of 1,045); 39.3% (11 of 28) involved the proximal stent edge, and 60.7% (17 of 28) involved the distal stent edge. In 50% (14 of 28), there was a sharply demarcated echolucent area within the hyperechoic hematoma, usually at the end opposite to the entry site that has been shown to correlate with angiographic contrast retention (Figs. 2 and 3). Extension of the intramural hematoma was limited by plaque or/and calcification in 19%, by a branch or vessel ostium in 52.4%, by a stent in 4.8%, and without an identifiable reason in 23.8%.

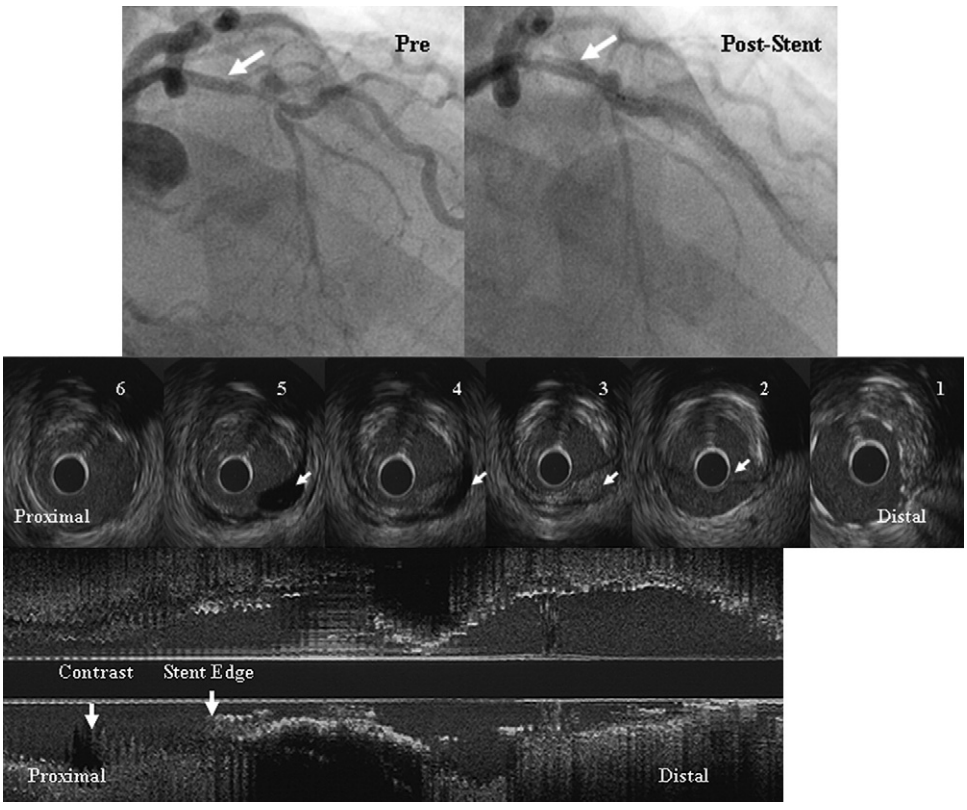

Figure 2. Intramural Hematoma With Contrast Retention

PAngiography showed type B dissection proximal to stent edge in the proximal left anterior descending coronary artery (**arrows** indicate dissection site on the pre- and post-stent angiograms). Intravascular ultrasound demonstrated an intramural hematoma with contrast retention; cross-sectional intravascular ultrasound images from 1 to 6 showed the hematoma start and stop sites. **1** = The proximal stent edge ended at an eccentric plaque. **2** = The hematoma developed in the arc of normal vessel wall opposite the eccentric plaque; note the thin intimal flap **(arrow)** adjacent to the intravascular ultrasound catheter. **3** = Smaller hematoma **(arrow)**. **4** = Small echolucent area **(arrow)** within the hematoma. **5** = Large echolucent area **(arrow)**. **6** = The proximal hematoma stop site.

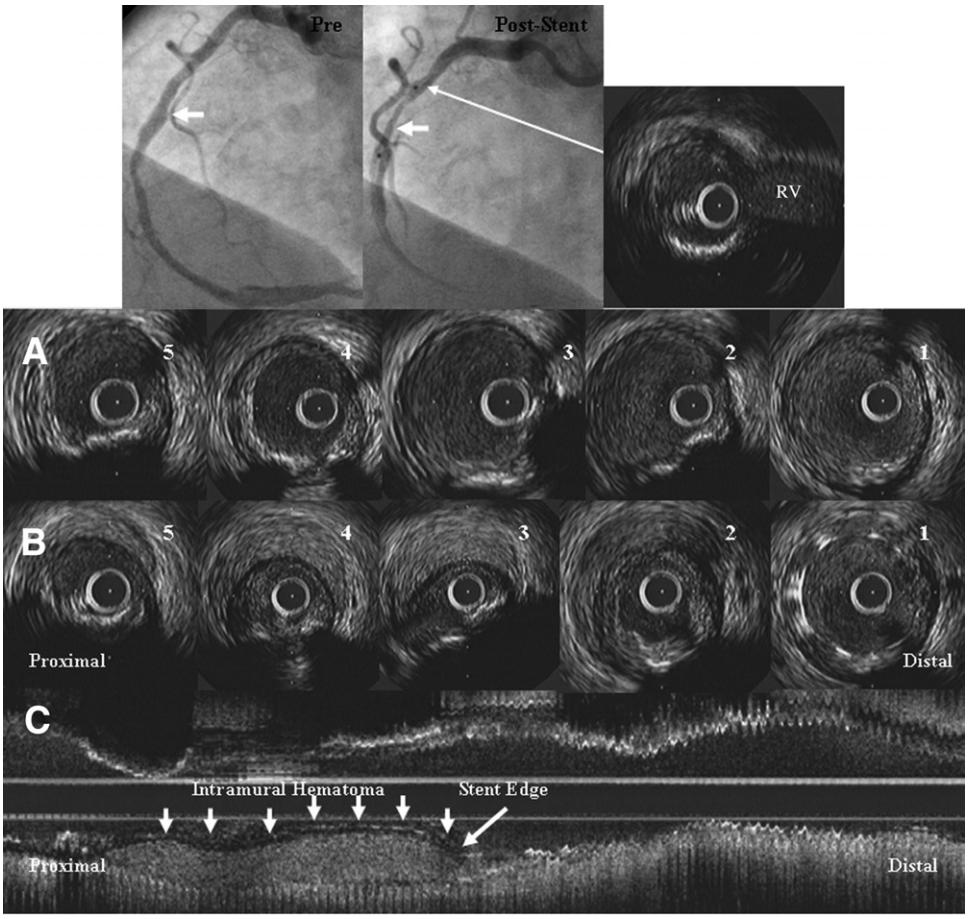

Figure 3. Intramural Hematoma Without Contrast Retention

Angiography showed type E dissection proximal to stent edge (**arrows** indicate dissection site on the pre- and post-stent angiograms) in the mid-right coronary artery. The cross-sectional intravascular ultrasound image showed that the hematoma was stopped by right ventricular (RV) branch. The intravascular ultrasound demonstrated an intramural hematoma without contrast retention. **(A)** The cross-sectional intravascular ultrasound images before stenting. **(B)** The cross-sectional intravascular ultrasound images after stent implantation showing a hematoma in sections **2** to **5**; individual cross sections correspond to the equivalent sections in **A**. **(C)** Longitudinal intravascular ultrasound image after stenting. **Long arrow** indicates the proximal stent edge and the hematoma start point that extended proximally. The intramural hematoma was 13.1 mm in length. **Short arrows** indicate the intramural hematoma without contrast retention.

Hematoma length and maximum hematoma CSA were 7.9 ± 3.3 mm and 3.9 ± 2.2 mm^2, respectively. When compared with opposite edges *without a dissection or hematoma*, a significant (≥50%) plaque burden was more common (50% vs. 15%, p = 0.01), P and M eccentricity was greater (8.4 ± 5.9 vs. 3.5 ± 3.2, p = 0.002), and calcium deposits (31.8% vs. 27.3%, p = 0.03) were more common at dissections with a hematoma. When stent edge dissections *with* an intramural hematoma were compared to edge dissections *without* a hematoma, there were no significant differences except that residual P and M area (6.4 ± 2.5 mm^2 vs. 8.9 ± 4.6 mm^2, p = 0.04) in the hematoma group was smaller and stent edges more symmetric (1.1 ± 0.1 vs. 1.2 ± 0.1, p = 0.009) (Table 4).

Predictors of stent edge dissection. Multivariable conditional logistic regression analysis showed that independent predictors of any stent edge dissection were residual plaque eccentricity (odds ratio [OR]: 1.4, 95% confidence interval [CI]: 1.1 to 1.9, p = 0.02), lumen-to-stent-edge-area ratio (OR: 0.00, 95% CI: 0.00 to 0.12, p = 0.007), and stent edge asymmetry (0.01-U) (OR: 1.2, 95% CI: 1.0 to 1.4, p = 0.02). Candidate variables for analysis were plaque morphology, calcium deposit, stent edge asymmetry, plaque eccentricity, mean-lumen-diameter-to-stent-diameter ratio, lumen-to-stent-edge-area ratio, P and M CSA, and significant plaque burden (≥50%).

Dissection treatment and 1-year follow-up. All patients with type B to F dissections and new stenoses were

Table 4. Dissections With Versus Without an Intramural Hematoma

	Dissection With Hematoma (n = 25)	Dissection Without Hematoma (n = 46)	p Value
Nominal stent diameter (mm)	3.2 ± 0.3	3.2 ± 0.5	0.82
Stent length (mm)	25.7 ± 13.7	22.6 ± 12.9	0.37
Maximum balloon size (mm)	3.3 ± 0.3	3.4 ± 0.5	0.38
Maximum dilation pressure (atm)	16.0 ± 3.7	16.3 ± 3.2	0.83
IVUS analysis			
Dissection length (mm)	7.9 ± 3.3	4.3 ± 2.3	<0.0001
Stent edge asymmetry	1.1 ± 0.1	1.2 ± 0.1	0.009
Mean reference/stent diameter	1.1 ± 0.1	1.0 ± 0.2	0.63
Peri-stent minimum lumen site			
Mean lumen diameter (mm)	3.1 ± 0.3	3.1 ± 0.4	0.61
Plaque eccentricity	8.4 ± 5.9	8.4 ± 5.3	0.97
Normal vessel arc (%)	23 (92.0)	36 (78.3)	0.14
P and M CSA (mm^2)	6.4 ± 2.5	8.9 ± 4.6	0.04
Plaque burden (%)	49.6 ± 10.2	54.0 ± 12.8	0.15
Most normal looking reference			
Mean lumen diameter (mm)	3.2 ± 0.4	3.3 ± 0.5	0.41
P and M CSA (mm^2)	5.9 ± 2.7	6.6 ± 3.7	0.30
Plaque burden (%)	42.3 ± 10.7	42.9 ± 11.5	0.15

Abbreviations as in Table 2.

treated with additional stents; conversely, 19 dissections (5 type A, 11 angiographic haziness, and 4 normal angiographic appearance) were left untreated. Overall, 77% (63 of 82) of dissections were treated with a total of 72 additional stents. One-year follow-up (median 367 days) was available in 86.6% of patients (71 of 82). During follow-up, there were 3 cardiac deaths (4.2%), 1 noncardiac death (1.4%), and a total of 4 repeat target lesion revascularizations (5.6%)—all in patients receiving additional stents to treat dissections.

Discussion

Balloon inflation and stent implantation are associated with mechanical dilation of the artery as well as plaque fracture, intimal splitting, and localized medial dissection that is a function of the biomechanical properties of the plaque (4,5). Stiffer atherosclerotic plaques resist circumferential expansion more than normal sites to generate high shear stresses at interfaces between stiff plaques and normal vessel segments to cause dissections (6). Richardson et al. (7) used computer modeling to predict intimal tears as a function of plaque composition; high tensile stresses occur at the junction between tissue types with differing elastic properties. The mechanism of post-stent dissections is similar to dissections caused by balloon dilation; the dissection occurs at the transition point between the rigid stent and the unstented reference segment—in other words, at the stent edge (8).

The angiographic incidence of coronary dissection after balloon angioplasty ranges from 32.4% to 50% (9,10). This decreases to 5% to 23% after stent implantation (8). Compared with the BMS era, DES implantation strategies may decrease the frequency of post-stent dissections (11,12). Persistent dissections after BMS may be associated with a worse prognosis including an increased risk of stent thrombosis (12–14).

IVUS detection of dissections and hematomas. IVUS identifies stent dissections and hematomas not detected by angiography (15,16). In the present study, 39% of the IVUS-identified dissections were not detected by angiography. In the pre-stent era, angiographic predictors included calcified lesions, eccentric lesions, long lesions, complex lesion morphology (American College of Cardiology/American Heart Association type B or C), vessel tortuousity, and a balloon-to-artery ratio >1.2 (17). Using IVUS, Fitzgerald et al. (16) reported that localized calcium deposits had a direct role in promoting dissection. Hong et al. (18) identified that plaque burden at dissection sites proximal or distal to BMS edge was significantly larger than at nondissection sites. Our findings were broadly concordant with previous IVUS findings; however, in the current study, the stent-vessel interface superceded the influence of different plaque components since superficial calcium was not a predictor of stent edge dissections.

An intramural hematoma begins as a dissection to the media and propagates along the medial plane into more normal arterial segments without re-entering the lumen (15). The thickness of the media behind atherosclerotic plaque is less than one-half that of the normal wall and is accompanied by scarring and loss of smooth muscle cells (19). Therefore, once medial dissection occurs, hematoma formation and expansion seem to require a normal segment or less-diseased arc of arterial wall because the media behind a large or hard plaque is more scarred and, therefore, limits propagation of the medial dissection.

Whether delayed healing and re-endothelialization seen after DES implantation influences healing of post-DES edge dissections has not been well studied. However, this issue has been investigated in patients treated with brachytherapy after which healing of coronary dissections is impaired (20–22).

Study limitations. Despite the fact that this is a large consecutive series of patients undergoing IVUS imaging during percutaneous intervention, there may be bias caused by patient selection, decision to use IVUS, or clinical decisions driven by the pre-intervention IVUS findings. However, these data were collected from a high-volume laboratory that utilizes IVUS routinely during interventional procedures. There was no control group of BMS-treated lesions.

JACC: CARDIOVASCULAR INTERVENTIONS, VOL. 2, NO. 10, 2009
OCTOBER 2009:997–1004

Conclusions

IVUS identified edge dissections after 9.2% of DES implantations and intramural hematomas after 3.2% of DES implantations. Residual plaque eccentricity, lumen-to-stent-edge-area ratio, and stent edge asymmetry predicted coronary stent edge dissections while dissections in less diseased reference segments more often evolved into an intramural hematoma.

Reprint requests and correspondence: Dr. Akiko Maehara, Cardiovascular Research Foundation, 111 East 59th Street, 12th Floor, New York, New York 10022. E-mail: amaehara@crf.org.

REFERENCES

1. Rogers JH, Lasala JM. Coronary artery dissection and perforation complicating percutaneous coronary intervention. J Invasive Cardiol 2004;16:493–9.
2. Holmes DR Jr., Holubkov R, Vlietstra RE, et al., for the Co-Investigators of the National Heart, Lung and Blood Institute Percutaneous Transluminal Coronary Angioplasty Registry. Comparison of procedural complications during percutaneous transluminal angioplasty from 1977 to 1981 and from 1985 to 1986: the National Heart, Lung and Blood Institute Percutaneous Transluminal Coronary Angioplasty Registry. J Am Coll Cardiol 1988;12:1149–55.
3. Mintz GS, Nissen SE, Anderson WD, et al. American College of Cardiology clinical expert consensus document on standards for acquisition, measurement and reporting of intravascular ultrasound studies. J Am Coll Cardiol 2001;37:1478–92.
4. Block P, Myler R, Stertzer S, et al. Morphology after transluminal angioplasty in human beings. N Engl J Med 1981;305:382–5.
5. Farb A, Virmani R, Atkinson JB, et al. Plaque morphology and pathologic changes in arteries from patients dying after coronary balloon angioplasty. J Am Coll Cardiol 1990;16:1421–9.
6. Lee RT, Kamm RD. Vascular mechanics for the cardiologist. J Am Coll Cardiol 1994;23:1289–95.
7. Richardson PD, Davies MJ, Born GVR. Influence of plaque configuration and stress distribution on fissuring of coronary atherosclerotic plaques. Lancet 1989;2:941–4.
8. Sheris SJ, Canos MR, Weissman NJ. Natural history of intravascular ultrasound-detected edge dissections from coronary stent deployment. Am Heart J 2000;139:59–63.
9. Baptista J, di Mario C, Ozaki Y, et al. Impact of plaque morphology and composition on the mechanisms of lumen enlargement using intracoronary ultrasound and quantitative angiography after balloon angioplasty. Am J Cardiol 1996;77:115–21.
10. Tenaglia AN, Buller CE, Kisslo KB, et al. Mechanisms of balloon angioplasty and directional coronary atherectomy as assessed by intracoronary ultrasound. J Am Coll Cardiol 1992;20:685–91.
11. Stankovic G, Chieffo A, Iakovou I, et al. Creatine kinase-myocardial band isoenzyme elevation after percutaneous coronary interventions using sirolimus-eluting stents. Am J Cardiol 2004;93:1397–401.
12. Biondi-Zoccai GGL, Agostoni P, Sangiorgi GM, et al. Incidence, predictors, and outcomes of coronary dissections left untreated after drug-eluting stent implantation. Eur Heart J 2006;27:540–6.
13. Cutlip DE, Baim DS, Ho KK, et al. Stent thrombosis in the modern era. A pooled analysis of multicenter coronary stent clinical trials. Circulation 2001;103:1967–71.
14. Cheneau E, Leborgne L, Mintz GS, et al. Predictors of subacute stent thrombosis: results of a systematic intravascular ultrasound study. Circulation 2003;108:2–5.
15. Maehara A, Mintz GS, Bui AB, et al. Incidence, morphology, angiographic finding, and outcomes of intramural hematomas after percutaneous coronary interventions: an intravascular ultrasound study. Circulation 2002;105:2037–42.
16. Fitzgerald PJ, Ports TA, Yock PG. Contribution of localized calcium deposits to dissection after angioplasty: an observational study using intravascular ultrasound. Circulation 1992;86:64–70.
17. Sharma SK, Israel DH, Kamean JL, et al. Clinical, angiographic, and procedural determinants of major and minor coronary dissection during angioplasty. Am Heart J 1993;126:39–47.
18. Hong MK, Park SW, Lee NH, et al. Long-term outcomes of minor dissections at the edge of stents detected with intravascular ultrasound. Am J Cardiol 2000;86:791–5.
19. Waller BF. The eccentric coronary atherosclerotic plaque: morphologic observations and clinical relevance. Clin Cardiol 1989;12:14–20.
20. Kay IP, Sabate M, Van Langenhove G, et al. Outcome of balloon induced coronary dissection after intracoronary beta radiation. Heart 2000;83:332–7.
21. Meerkin D, Tardif JC, Bertrand OF, et al. The effects of intracoronary brachytherapy on the natural history of postangioplasty dissections. J Am Coll Cardiol 2000;36:59–64.
22. McClean DR, Thomas MR. Non-flow limiting dissection leading to late coronary restenosis following intracoronary brachytherapy. Cathet Cardiovasc Intervent 2001;54:355–7.

Key Words: drug-eluting stent ■ intravascular ultrasound ■ edge dissection ■ intramural hematoma.